A novel design of dual-band bandstop waveguide filter using split ring resonators

S. Lj. STEFANOVSKI*, M. M. POTREBIĆ[a], D. V. TOŠIĆ[a]
Ph.D. student, School of Electrical Engineering, University of Belgrade, P.O. Box 35-54, 11120 Belgrade, Serbia; Telekom Srbija, Bulevar umetnosti 16, 11070 Belgrade, Serbia
[a]*School of Electrical Engineering, University of Belgrade, P.O. Box 35-54, 11120 Belgrade, Serbia*

A novel bandstop waveguide filter, using split ring resonators, is proposed. Split ring resonators are implemented as printed-circuit inserts in a form of reduced dielectric plates, providing better performance in terms of return loss beyond the stop band, compared with the structure where dielectric plates across the entire transverse cross-section are applied. The filter response is analyzed depending on the various parameters of the resonators. These resonators are used for the design of third-order bandstop waveguide filter for single resonant frequency. Also, a novel design of multi-band bandstop waveguide filter is developed and dual-band bandstop waveguide filter of the third order, using split ring resonators, is presented as an example.

(Received July 21, 2013; accepted March 13, 2014)

Keywords: Bandstop waveguide filter, Dual-band bandstop waveguide filter, Multi-band filter, Split ring resonators

1. Introduction

Waveguide filters play a significant role in microwave and millimetre-wave applications, where low-loss and high power structures need to be implemented. Their principle of operation is based on the insertion of the discontinuities acting as resonators [1]. Split ring resonators (SRRs) and complementary split ring resonators (CSRRs) have wide implementation for bandstop and bandpass filter design, respectively, either as single-band or multi-band. Multi-band filters are particularly interesting for consideration.

Previously published papers have reported various methods for filter realization using SRRs and CSRRs. Bandpass filters with CSRRs, realized in microstrip technology with defected ground structure, are presented in [2-3], although there are also realizations using substrate integrated waveguide [4] or using rectangular waveguide [5-7]. Similarly, bandstop waveguide filter with SRRs is proposed in [8]. A common feature of all mentioned structures is single frequency band.

Various examples of CSRRs and SRRs, realized as printed-circuit inserts in the rectangular waveguide, are presented in [9] and [10-12], for the design of multi-band bandpass and bandstop filters, respectively.

In this paper, novel SRRs, in the form of reduced dielectric plates, supported by thin dielectric strips, are designed and implemented as printed-circuit inserts in the rectangular waveguide. Standard WR90 rectangular waveguide is used, and SRRs are inserted in the transverse planes, in order to obtain H-plane bandstop waveguide filter. By choosing the proper position of the SRRs, third-order Chebyshev filters are designed for the resonant frequencies of 9 GHz and 11 GHz. Finally, dual-band Chebyshev bandstop waveguide filter of the third order is designed. This filter covers two resonant frequencies (f_{01} = 9 GHz, f_{02} = 11 GHz), i.e. it has two stop bands, each of which has a bandwidth of 335 MHz. For the design and analysis of the considered structures, software supporting three-dimensional full-wave electromagnetic simulations is used.

The objective of this research was to design novel SRRs, to model the bandstop waveguide filters using these SRRs and analyze filter responses depending on various parameters of the SRRs. Also, third-order filters are modelled and their responses are compared with those of the proposed equivalent circuits. A novel design of multi-band bandstop waveguide filter is developed. Based on that, third-order dual-band bandstop waveguide filter, using proper combination of the novel SRRs, is introduced.

2. Bandstop waveguide filter using novel SRRs

The design of the bandstop waveguide filter started from the previously proposed model [10-11], using SRRs designed on a dielectric plate which covers the entire transverse cross-section of the waveguide. Novel SRRs are modelled in the form of reduced dielectric plates, supported by thin dielectric strips, and they are inserted in the rectangular waveguide. These SRRs are used for the design of the bandstop waveguide filters with resonant frequencies of 9 GHz and 11 GHz. The three-dimensional (3D) electromagnetic (EM) model of the filter using novel SRRs is depicted in Fig. 1. The parameters of the resonators are tuned by means of a series of simulations in WIPL-D software [13], in order to obtain proper resonant frequency and bandwidth.

For the filter design, the WR90 standard rectangular waveguide of width a = 22.86 mm and height

b = 10.16 mm is used. It is assumed that the dominant mode of propagation is the transverse electric TE_{10} mode. The waveguide filter is excited by quarter-wave monopoles, modelled as thin wires with ideal voltage sources at the wire-to-plate junction positions. The excitations realized in this manner are parts of the waveguide structure. In order to be able to calculate the filter response accurately, i.e. to obtain only the *s*-parameters of the filter, the de-embedding technique, based on reflection coefficient measurements, is applied. The method is performed in three steps, as described in [14], which can be summarized as follows. First, the *s*-parameters of the full network are obtained by means of WIPL-D simulation. Then, feeding circuits (ports) are properly modelled and analyzed separately, and their *s*-parameters are also obtained by means of WIPL-D simulations. Finally, when the *s*-parameters of the complete structure and the feeding circuits are available, the *s*-parameters of the desired structure (in our case, waveguide filter) can be easily obtained by applying the de-embedding option of the WIPL-D software.

The printed-circuit inserts are realized on RT/Duroid 5880 microstrip board with a thickness of h = 0.8 mm and a metallization thickness of t = 0.018 mm. Each printed-circuit insert consists of the dielectric plate of width a_{pl} = 7 mm and height b_{pl} = 4 mm, supported by dielectric strips of width w_{str} = 0.4 mm. According to Fig. 1, the parameters of the SRRs are given in Table 1. The SRR used here for the bandstop waveguide filter design has the gap on the right side of the ring. In [11], the filter response is analyzed for different positions of the SRR, and it has been concluded that the filter has bandstop characteristic only for two positions of the SRR, i.e. when the gap is on the left and right side of the ring. For the other two positions (when the gap is facing up and down), the waveguide with the printed-circuit insert does not operate as a bandstop filter.

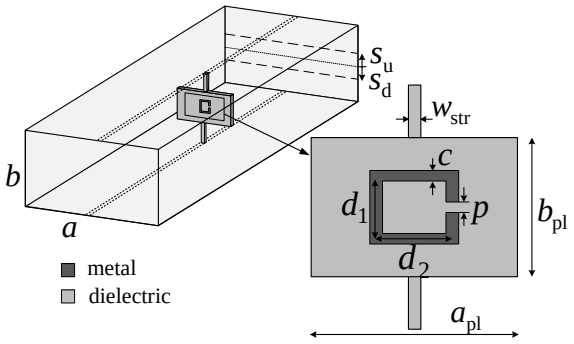

Fig. 1. 3D EM model of the rectangular bandstop waveguide filter using novel SRR.

Table 1. Dimensions of the novel SRRs.

Resonant frequency	d_1 [mm]	d_2 [mm]	c [mm]	p [mm]
f_0 = 9 GHz	2.5	4.9	0.2	0.9
f_0 = 11 GHz	2.5	3.6	0.2	0.9

The WIPL-D model of the considered waveguide filter, along with the model of the feeding structure, is shown in Fig. 2. The obtained filter response, compared with the response of the filter with dielectric plate across the entire transverse cross-section as in [10-11], is shown in Fig. 3. It should be emphasized that the dimensions of the metallic strip (length and width) are the same for these two models.

From the presented results, it can be noticed that the resonant frequencies are slightly moved apart, but the return loss has lower values beyond the stop band for the model with reduced printed-circuit inserts, compared with the same parameter for the model with dielectric plates across the entire transverse cross-section.

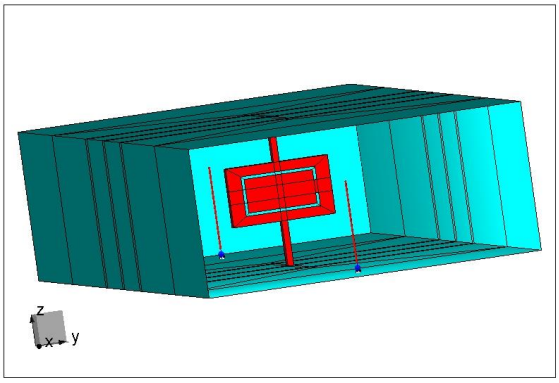

(a)

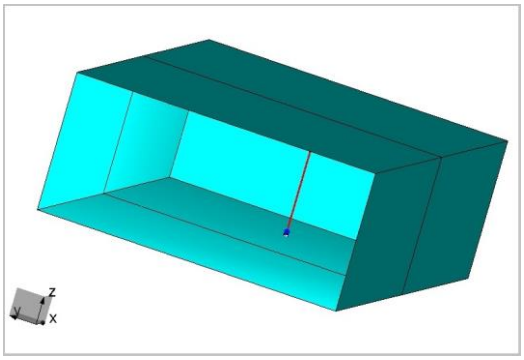

(b)

Fig. 2. WIPL-D model of: (a) the rectangular bandstop waveguide filter using novel SRR, (b) the feeding structure.

The influence of the parameters of the SRR on the filter response is investigated. The variation of the resonant frequency with the length of the metallic strip is shown in Fig. 4. As can be seen, the resonant frequency moves towards the higher values, as the length of the strip (d_2) decreases. Further, the influence of the strip width is also investigated. It is noticed that the variation of the strip width primarily influences the bandwidth, while the frequency shift is practically negligible. Therefore, the bandwidth variation is of interest in this case and these results are shown in Fig. 5.

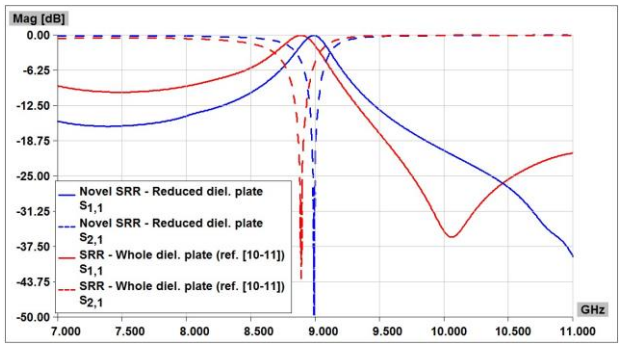

(a)

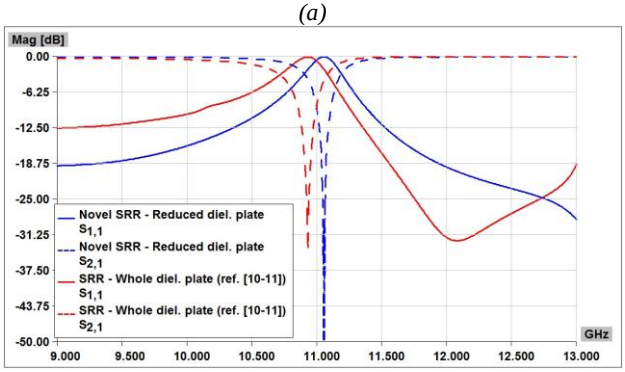

(b)

Fig. 3. Comparison of filter responses (filter with novel SRR and previously proposed SRR as in [10-11]): (a) f_0 = 9 GHz, (b) f_0 = 11 GHz.

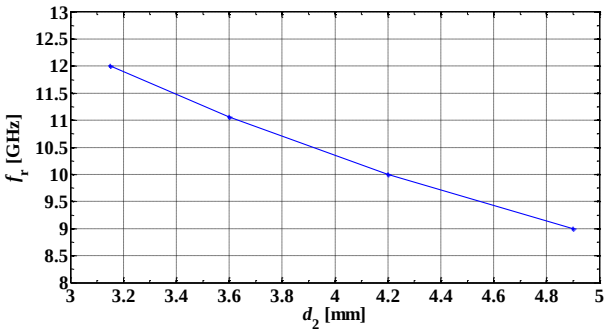

Fig. 4. The resonant frequency variation with strip length: d_1 = 2.5 mm, c = 0.2 mm, p = 0.9 mm, d_2 varies.

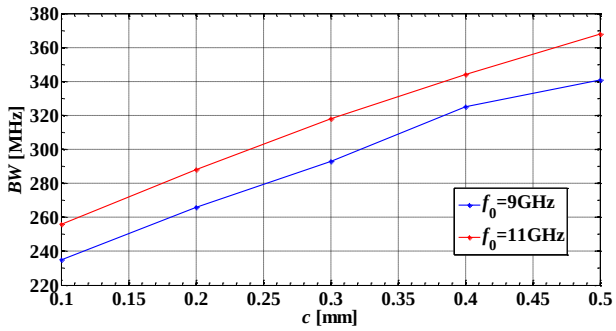

Fig. 5. The bandwidth variation with strip width: d_1 = 2.5 mm, d_2 = 4.9 mm (f_0 = 9 GHz), d_2 = 3.6 mm (f_0 = 11 GHz), p = 0.9 mm, c varies.

Finally, the influence of the printed-circuit insert position is analyzed. Namely, the dielectric plate is moved up and down, related to the central position, and the filter responses are compared. These results are given in Fig. 6 for the case when the plate is moved up and down for $s_u = s_d = 2.85$ mm related to the central position. The obtained results show that, for the chosen length of the metallic strip, the resonant frequency of the bandstop filter can be tuned by moving the plate up and down, without changing the bandwidth. This conclusion is important for further design of the filter with chosen resonant frequencies. Namely, the separation of the SRRs is considered in order to achieve negligible coupling between them in case when several resonators are realized on the same plate.

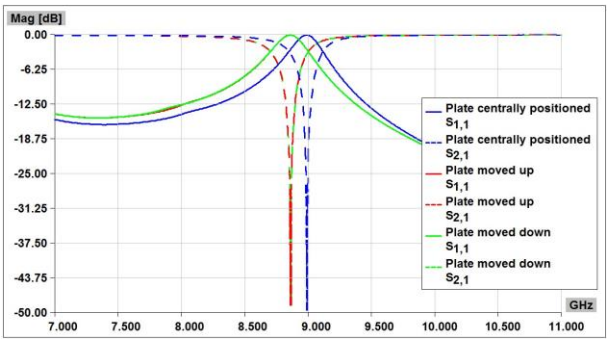

(a)

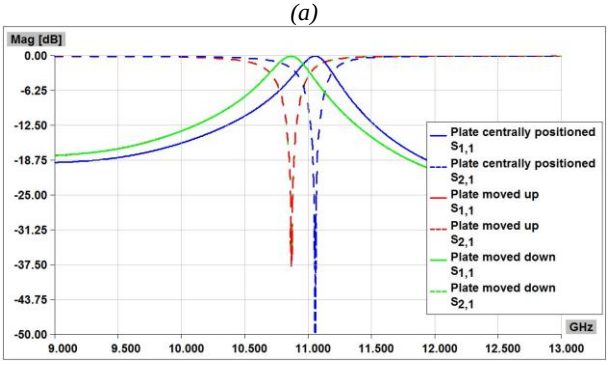

(b)

Fig. 6. The resonant frequency variation with plate position: (a) f_0 = 9 GHz, (b) f_0 = 11 GHz.

3. Third-order bandstop waveguide filters using novel SRRs

The novel SRRs are used for the design of the third-order bandstop waveguide filters with the resonant frequencies of 9 GHz and 11 GHz. Filters are modelled using Chebyshev approximation starting from the lowpass prototype, then the lowpass to bandstop transformation is applied. Since the parallel resonant circuits are of interest, the inverters are implemented in the equivalent circuit and the L and C parameters of the resonators are determined, as proposed in [15]. The parameters of the SRRs, modelled in software WIPL-D, are tuned in order to achieve good agreement with the response of the equivalent circuit, in terms of resonant frequency and bandwidth.

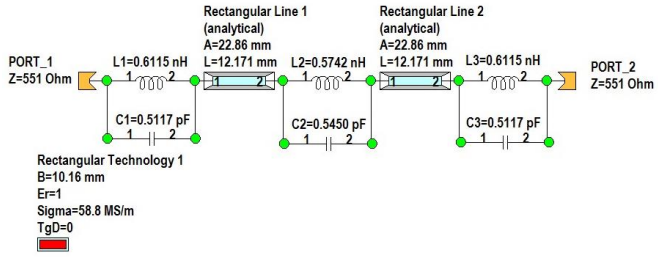

Fig. 7. Equivalent circuit of the third-order rectangular bandstop waveguide filter.

First, the third-order Chebyshev bandstop filter for f_0 = 9 GHz is designed. Equivalent circuit is modelled using WIPL-D software and it is shown in Fig. 7, along with the values of L and C parameters. The port impedance corresponds to the wave impedance (Z_{TE}) of the waveguide for the chosen resonant frequency. For f_0 = 9 GHz, Z_{TE} = 551 Ω. The "Rectangular Line" component, representing the waveguide section of the proper length, is inserted between the resonators in the equivalent circuit, in order to emulate the inverters in the 3D EM model. The 3D EM model of the filter using novel SRRs is depicted in Fig. 8. For the WIPL-D model (Fig. 9), dielectric plates are moved up for s_u = 2.85 mm related to central position and the parameters of the resonators (Table 2) are tuned in order to obtain required resonant frequency of 9 GHz. Each plate is of the same size (7 mm × 4 mm). The plates are mutually separated by the distance of $\lambda_{g\,9GHz}$ / 4 = 12.171 mm, in order to realize quarter-wave immittance inverters between the resonators, for the corresponding resonant frequency.

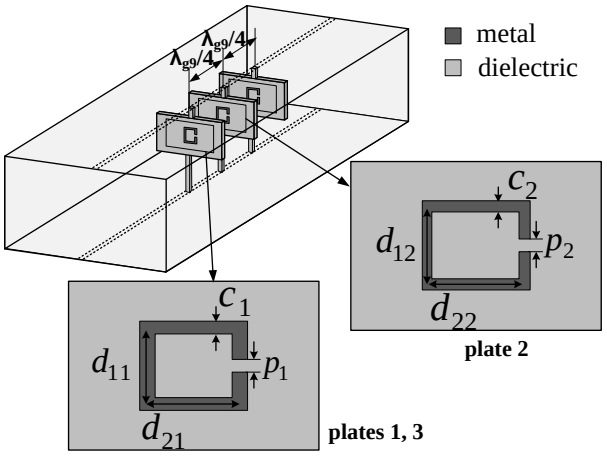

Fig. 8. 3D EM model of the third-order rectangular bandstop waveguide filter using novel SRRs.

Table 2. Dimensions of the SRRs for the third order bandstop waveguide filter with f_0 = 9 GHz.

Dimension	d_{1i} [mm]	d_{2i} [mm]	c_i [mm]	p_i [mm]
First/third plate (i=1,3)	2.50	4.75	0.18	0.90
Second plate (i=2)	2.50	4.75	0.16	0.90

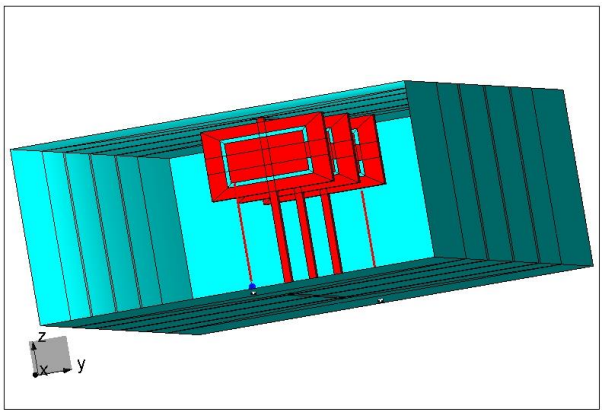

Fig. 9. WIPL-D model of the third-order rectangular bandstop waveguide filter using novel SRRs.

The filter responses are compared for the equivalent circuit and 3D EM model made in WIPL-D software, and relatively good agreement is achieved in terms of resonant frequency and bandwidth (Table 3), as can be seen in Fig. 10.

Table 3. Numerical results for 3D EM model and equivalent circuit of the bandstop waveguide filter with f_0 = 9 GHz.

Realization	f_0 [GHz]	B_{3dB} [MHz]
3D EM model	9.062	333
Equivalent circuit	8.995	335

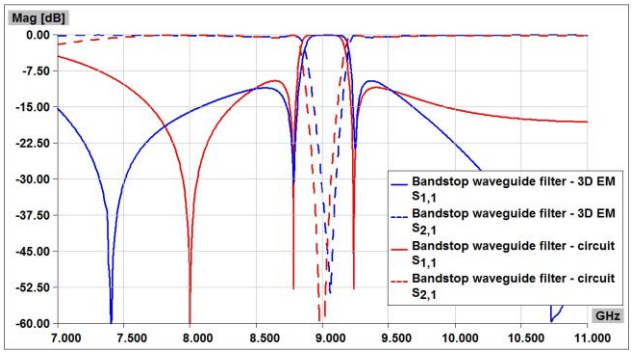

Fig. 10. Comparison of filter responses for the equivalent circuit and 3D EM model (f_0 = 9 GHz).

Next, the third-order Chebyshev bandstop filter for f_0 = 11 GHz is designed. Following the same procedure as for the previous model, the equivalent circuit is realized and is shown in Fig. 11, along with the values of L and C

parameters. For this model, $Z_{TE} = 470\ \Omega$. The 3D EM model of the filter using novel SRRs is depicted in Fig. 12. For the WIPL-D model (Fig. 13), dielectric plates are moved down for $s_d = 2.85$ mm related to the central position and the parameters of the resonators (Table 4) are tuned in order to obtain required resonant frequency of 11 GHz. Each plate is of the same size (7 mm × 4 mm). The plates are mutually separated by the distance of $\lambda_{g\ 11GHz}/4 = 8.494$ mm.

The filter responses are compared for the equivalent circuit and 3D EM model made in WIPL-D software, and relatively good agreement is achieved in terms of resonant frequency and bandwidth (Table 5), as can be seen in Fig. 14.

Table 4. Dimensions of the SRRs for the third-order bandstop waveguide filter with $f_0 = 11$ GHz.

Dimension	d_{1i} [mm]	d_{2i} [mm]	c_i [mm]	p_i [mm]
First/third plate (i=1,3)	2.50	3.53	0.40	0.90
Second plate (i=2)	2.50	3.53	0.36	0.90

Table 5. Numerical results for 3D EM model and equivalent circuit of the bandstop waveguide filter with $f_0 = 11$ GHz.

Realization	f_0 [GHz]	B_{3dB} [MHz]
3D EM model	11.037	333
Equivalent circuit	11.005	334

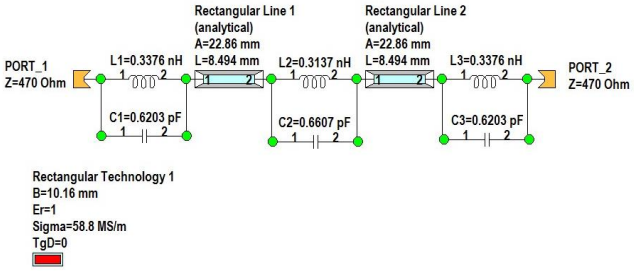

Fig. 11. Equivalent circuit of the third-order rectangular bandstop waveguide filter.

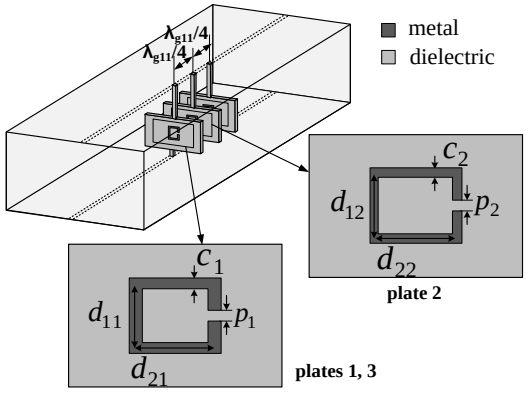

Fig. 12. 3D EM model of the third-order rectangular bandstop waveguide filter using novel SRRs.

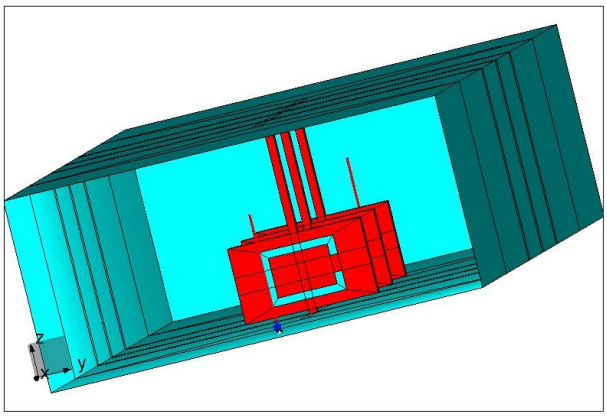

Fig. 13. WIPL-D model of the third-order rectangular bandstop waveguide filter using novel SRRs.

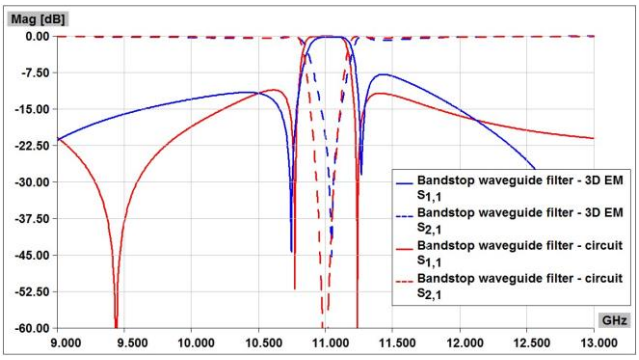

Fig. 14. Comparison of filter responses for the equivalent circuit and 3D EM model ($f_0 = 11$ GHz).

4. Third-order dual-band bandstop waveguide filter using novel SRRs

Based on the novel design of the multi-band bandstop waveguide filter, dual-band bandstop filter is modelled. Namely, the third-order filters presented in the previous section are used for the design of the third-order dual-band bandstop waveguide filter. The idea is to use corresponding SRRs and place them at the proper positions in the waveguide, in order to obtain dual-band filter with resonant frequencies $f_{01} = 9$ GHz and $f_{02} = 11$ GHz.

The equivalent circuit of the dual-band filter is shown in Fig. 15. The values of the L and C parameters are the same as those used in the circuits for each of the considered filters. In this case, the value of the port impedance is $Z = 500\ \Omega$. This value corresponds to the wave impedance (Z_{TE}) of the waveguide with the resonant frequency of $f_0 = 10$ GHz, which is the frequency between the considered ones (9 GHz and 11 GHz).

The 3D EM model of the novel dual-band bandstop waveguide filter is depicted in Fig. 16. The SRRs are placed at the same positions as in each individual filter, i.e. the proper distances between the resonators are applied: the SRRs for $f_{01} = 9$ GHz are mutually separated by

$\lambda_{g\,9GHz}/4 = 12.171$ mm, and those for $f_{02} = 11$ GHz are separated by $\lambda_{g\,11GHz}/4 = 8.494$ mm. According to this, the distance between the SRRs for different resonant frequencies is $(\lambda_{g\,9GHz}-\lambda_{g\,11GHz})/4 = 3.677$ mm. Next, it is important to emphasize that the dimensions of the SRRs are the same as for the described filters and are given in Tables 2 and 4. Related to the central position in the transverse planes, the SRRs for $f_{01} = 9$ GHz are moved up for $s_u = 2.85$ mm, and those for $f_{02} = 11$ GHz are moved down for $s_d = 2.85$ mm. This is done in order to eliminate the mutual coupling between the SRRs placed in the same transverse plane. The WIPL-D model of the dual-band filter is shown in Fig. 17.

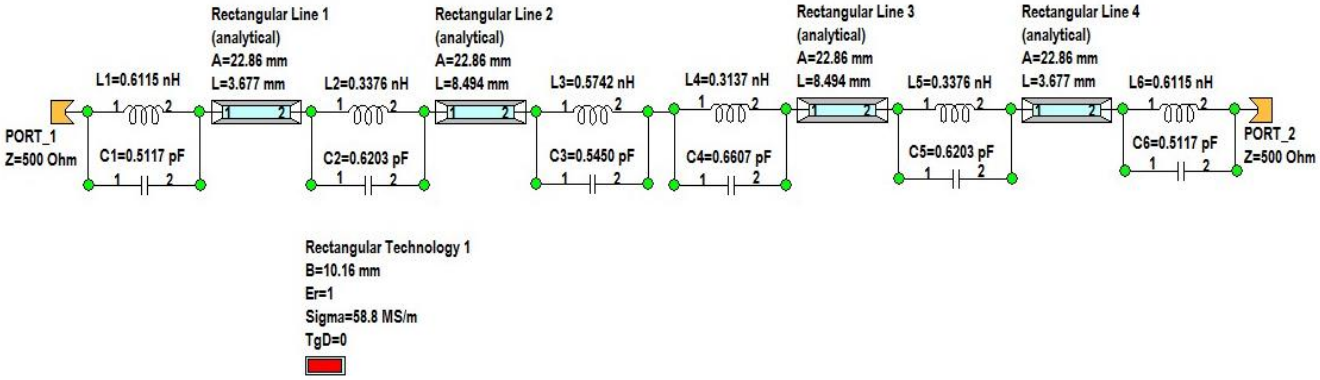

Fig. 15. Equivalent circuit of the dual-band third-order rectangular bandstop waveguide filter.

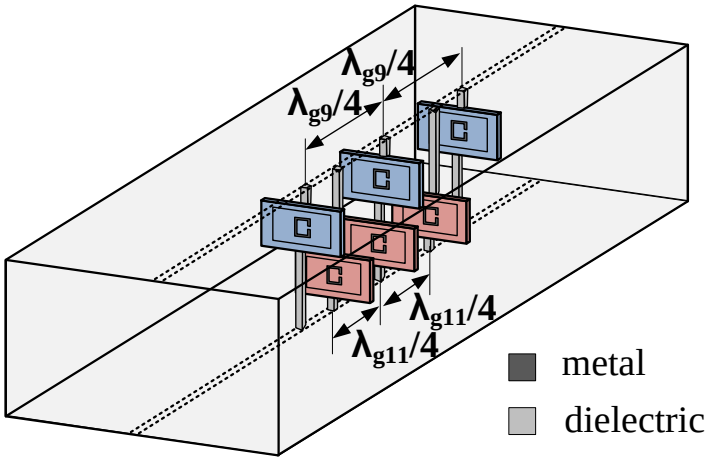

Fig. 16. 3D EM model of the dual-band third-order rectangular bandstop waveguide filter using novel SRRs.

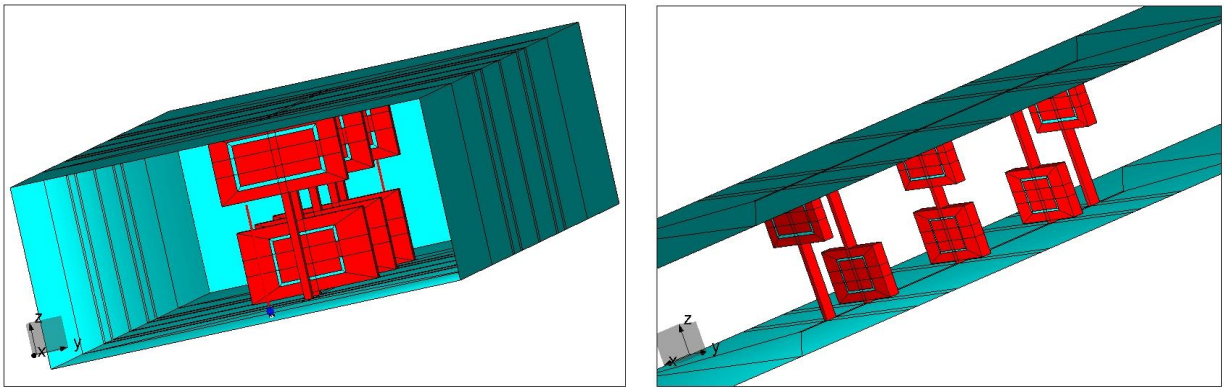

(a) *(b)*

Fig. 17. WIPL-D model of the dual-band third-order rectangular bandstop waveguide filter using novel SRRs: (a) waveguide filter, (b) layout of the SRRs.

Table 6. Numerical results for 3D EM model and equivalent circuit of the dual-band bandstop waveguide filter.

Realization	1. stopband		2. stopband	
	f_0 [GHz]	B_{3dB} [MHz]	f_0 [GHz]	B_{3dB} [MHz]
3D EM model	9.036	340	11.031	332
Equivalent circuit	9.010	325	11.024	337

The dual-band filter response is compared with that obtained by the equivalent circuit. This is shown in Fig. 18. As can be seen, the design requirements are accomplished in terms of the resonant frequencies and the bandwidth and the results are matched relatively good. Numerical results are given in Table 6. Also, the response of the dual-band filter is compared with the responses of individual single-band filters and these results are given in Fig. 19. There is good agreement between the obtained responses. Thus, it can be concluded that dual-band filter can be independently tuned for each of the resonant frequencies, which is important for the design of multi-band filters.

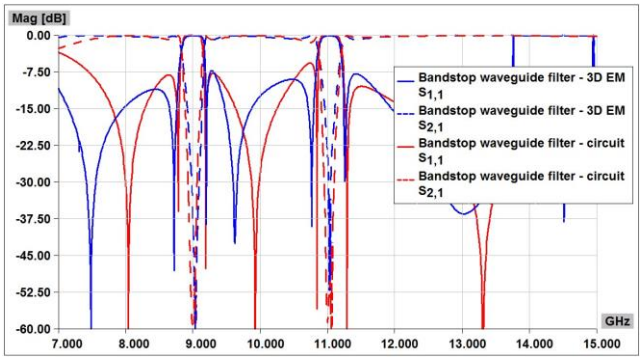

Fig. 18. Comparison of filter responses for the equivalent circuit and 3D EM model of the dual-band third-order bandstop waveguide filter using novel SRRs.

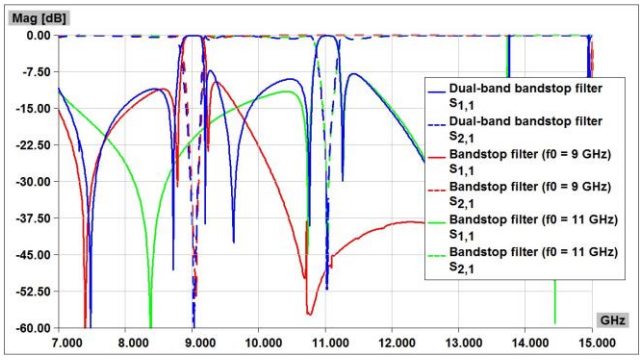

Fig. 19. Comparison of filter responses for the dual-band filter and filters for each particular resonant frequency.

5. Conclusion

Novel SRRs are proposed for the design of the bandstop waveguide filters. They provide better performance in terms of return loss beyond the stop band, compared with the previously introduced structure with dielectric plates across the entire transverse cross-section. The influence of the parameters of the SRR on the filter response has been investigated and it is concluded that the length of the SRR primarily influences the resonant frequency, while the width mainly affects the bandwidth of the stop band. Also, the position of the SRR in the transverse plane has been analyzed and it is shown that, by moving the plate, the resonant frequency can be tuned, without changing other parameters of the SRR. Novel SRRs are then implemented for modelling of the third-order waveguide filters. The required resonant frequencies and bandwidths are obtained, and good agreement is achieved between the responses of the equivalent circuit and 3D EM model. Finally, as an example of proposed design of multi-band bandstop waveguide filters, dual-band third-order bandstop waveguide filter is modelled by choosing the proper positions of the novel SRRs. The obtained resonant frequencies and bandwidths are matched relatively good with those obtained by the equivalent circuit. Also, the response of the dual-band filter is compared with the responses of the previously described single-band bandstop filters. Practically the same resonant frequencies and bandwidths have been accomplished, which was our targeted result. This is important conclusion, because the proposed filter design allows independent control of each band for multi-band filters.

Acknowledgments

This work was supported by the Ministry of Education, Science and Technological Development of the Republic of Serbia under Grant TR32005.

References

[1] I. C. Hunter, Theory and Design of Microwave Filters, IET, London (2006).
[2] J. Bonache, F. Martin, F. Falcone, J. D. Baena, T. Lopetegi, J. Garcia-Garcia, M. A. G. Laso, I. Gil, A. Marcotegui, R. Marques, M. Sorolla, Microw. Opt. Techn. Lett. **46**, 508 (2005).
[3] J. Bonache, F. Martin, I. Gil, J. Garcia-Garcia, R. Marques, M. Sorolla, Microw. Opt. Techn. Lett. **46**, 343 (2005).
[4] X. C. Zhang, Z. Y. Yu, J. Xu, Prog. Electromagn. Res.

72, 39 (2007).
[5] N. Ortiz, J. D. Baena, M. Beruete, F. Falcone, M. A. G. Laso, T. Lopetegi, R. Marques, F. Martin, J. Garcia-Garcia, M. Sorolla, Microw. Opt. Techn. Lett. **46**, 88 (2005).
[6] H. Bahrami, M. Hakkak, Prog. Electromagn. Res. **80**, 107 (2008).
[7] M. M. Potrebić, D. V. Tošić, Z. Ž. Cvetković, N. Radosavljević, Proc. 28-th Intern. Conf. Microelectron., Niš, Serbia, IEEE – ED/SSC Chapter, 2012, p. 309.
[8] S. Fallahzadeh, H. Bahrami, M. Tayarani, Electromagnetics **30**, 482 (2010).
[9] S. Lj. Stefanovski, M. M. Potrebić, D. V. Tošić, Proc. 11-th Intern. Conf. Telecommun. Mod. Satell. Cable Broadcast. Serv., Niš, Serbia, Faculty of Electronic Engineering, 2013, p. 257.
[10] S. Fallahzadeh, H. Bahrami, M. Tayarani, Prog. Electromagn. Res. Let. **12**, 133 (2009).
[11] S. Lj. Stefanovski, M. M. Potrebić, D. V. Tošić, Z. Ž. Cvetković, Proc. 11-th Intern. Conf. Appl. Electromagnetics, Niš, Serbia, Faculty of Electronic Engineering, 2013, p. 135.
[12] M. N. M. Kehn, O. Quevedo-Teruel, E. Rajo-Iglesias, Electron. Lett. **44**, 714 (2008).
[13] WIPL-D Pro 10.0, 3D Electromagnetic Solver, WIPL-D d.o.o., Belgrade, Serbia (2012).
[14] B. Kolundžija, J. Ognjanović, M. Tasić, D. Olćan, M. Božić, M. Kostić, M. Pavlović, B. Mrdaković, T. Milošević, S. Marić, Đ. Petrović, D. Zorić, D. Jeremić, M. Kovač, N. Timko: WIPL-D Pro v10.0 3D Electromagnetic Solver Professional Edition – User's Manual, WIPL-D d.o.o., Belgrade, Serbia (2012).
[15] J.-S. Hong, Microstrip Filters for RF/Microwave Applications, Wiley, New York (2011).

*Corresponding author: snezanastef@telekom.rs